PROCEEDINGS, 45th Workshop on Geothermal Reservoir Engineering
Stanford University, Stanford, California, February 10-12, 2020
SGP-TR-216

Spatio–Temporal Analysis of Deformation at San Emidio Geothermal Field, Nevada, USA between 1992 and 2010

Kurt L. FEIGL[1], Elena C. REINISCH[1,5], Samuel A. BATZLI[1], Hiroki SONE[1], Michael A. CARDIFF[1], Jesse C. HAMPTON[1], Neal E. LORD[1], Clifford H. THURBER[1], Herbert F. WANG[1], Christopher SHERMAN[2], Christina MORENCY[2], Ian WARREN[3], Corné KREEMER[4]

(1) University of Wisconsin-Madison, 1215 West Dayton Street, Madison, WI, 53706 USA. http://geoscience.wisc.edu;
(2) Lawrence Livermore National Laboratory https://www.llnl.gov;
(3) National Renewable Energy Laboratory (NREL) https://www.nrel.gov;
(4) University of Nevada, Reno, USA http://www.nbmg.unr.edu;
(5) Los Alamos National Laboratory, USA https://www.lanl.gov

feigl@wisc.edu

Keywords: InSAR, GPS, radar

ABSTRACT

Deformation has been observed at San Emidio geothermal field in Nevada using geodetic and seismic instruments. These observations point to an interaction between operations at the power plant and stress in the subsurface. In particular, cooling of the reservoir (via injected cooled water) and localized pressure changes (due to pumping and injection) contribute to the stress state at San Emidio.

Our WHOLESCALE proposal has been recommended by the Geothermal Technologies Office of the U.S. Department of Energy for negotiation of a financial award. Indeed, the WHOLESCALE acronym stands for "Water & Hole Observations Leverage Effective Stress Calculations And Lessen Expenses". The goal of the WHOLESCALE project is to simulate the spatial distribution and temporal evolution of stress in a geothermal system. To reach this goal, the WHOLESCALE team proposes to develop a methodology that will incorporate and interpret data from four methods of measurement into a multi-physics model that couples thermal, hydrological, and mechanical (T-H-M) processes over spatial scales ranging from the diameter of a borehole (~0.1 m) to the extent of the entire field (~10 km) and temporal scales ranging from the duration of a micro-seismic event (~1 second) to the typical lifetime of a producing field (3 decades).

1. INTRODUCTION: SAN EMIDIO GEOTHERMAL FIELD, NEVADA, USA

The San Emidio geothermal area is located ~100 km north of Reno Nevada in the northwestern Basin and Range province. The San Emidio geothermal system occupies a right step in a North-striking, West-dipping, normal fault zone. Minor dilation and high fault density within the right step likely produce the permeability necessary for deep fluid circulation [*Eneva et al.*, 2011]. Power was first produced in 1987 with a 3.6 MW binary plant, and average production increased to 9 MW (net) following commissioning of a new power plant in 2012. Production has ranged from less than 190 L/s to more than 280 L/s at temperatures of 140–148˚C. Drilling, geological, geophysical, and geochemical data sets collected since the 1970s help constrain controls on the geothermal resource and the structural setting (Figure 1). In 2016, drilling south of the producing field discovered a new resource.

As described below, the geothermal field at San Emidio provides an ideal laboratory for understanding subsurface stress. The data collected over more than 20 years of operating experience characterize the structure, temperature, microseismicity, and permeability, all of which are directly associated with changes in the stress within the geothermal system. The data sets include: historic drilling records, magnetotelluric resistivity, seismic reflection imaging, passive seismic emission tomography (PSET), microseismicity analysis, and gravimetric surveys.

At San Emidio, a DOE-sponsored project (DOE award DE-EE0002847) conducted exploratory drilling between 2010 and 2014 and found the following results: "Five of the southern exploration wells encountered temperatures above the commercial target temperature of 280ºF [138ºC]. Three of the seven wells encountered both commercially exploitable temperature and permeability… This result confirms the existence of a thermal anomaly of higher temperature as compared to the existing wellfield extending southwestward from the southernmost exploration well." [*Teplow and Warren*, 2015].

A second DOE-sponsored project has been underway at San Emidio since 2016 as part of DOE's Subsurface Technology and Engineering R&D (SubTER) Crosscut program. Entitled "A Novel Approach to Map Permeability Using Passive Seismic Emission Tomography" (award DE-EE0007698), this project seeks to characterize the geothermal resource at San Emidio. The permeability associated with the newly discovered resource south of the producing field coincides with energy anomalies defined by passive seismic emission tomography (PSET) and with low-resistivity anomalies in the electromagnetic data [*Warren et al.*, 2018].

By analyzing these data streams, we can take advantage of the perturbations created by pumping operations to infer temporal changes in the state of stress in the geothermal system. For example, we conducted the PoroTomo experiment at the geothermal field at Brady Hot Springs, Nevada [*Feigl et al.*, 2019]. There, a scheduled cessation of both production and injection pumping produced fluid pressure changes as large as 150 kPa (roughly equivalent to 15 m of water) [*Patterson et al.*, 2017] that are associated with microseismic events [*Cardiff et al.*, 2018]. There, "shutdowns in pumping for plant maintenance correlate with increased microseismicity" [*Cardiff et al.*, 2018]. Following these authors, we hypothesize that "extraction of fluids inhibits fault slip by increasing the effective [normal] stress on faults; in contrast, brief pumping cessations represent times when effective [normal] stress is decreased below its long-term average, increasing the likelihood of microseismicity" [*Cardiff et al.*, 2018].

Similar phenomena have been observed at San Emidio. In the month of December 2016, more than 100 discrete micro-seismic events occurred as the power plant and pumping were shut down and subsequently restarted [*Warren et al.*, 2018]. These events are related temporally to recovery during shutdown and spatially clustered around the producing wells.

Observations elsewhere also indicate that anthropogenic perturbations to hydrological systems can alter the state of stress sufficiently to trigger seismic slip on pre-existing faults [e.g., *Raleigh et al.*, 1976; *Ellsworth*, 2013; *Segall and Lu*, 2015]. Similarly, extracting and injecting brine out of and into geothermal fields can also induce seismicity, especially in enhanced geothermal systems (EGS) [*Majer et al.*, 2007; *Brodsky and Lajoie*, 2013; *NRC*, 2013; *Kwiatek et al.*, 2015; *McGarr et al.*, 2015; *Trugman et al.*, 2016].

Such induced seismicity is caused by changes to the state of stress in and around the geothermal reservoir. Indeed, we hypothesize that increasing pore-fluid pressure reduces the effective normal stress acting across preexisting faults and induces micro-seismic events.

WHOLESCALE PROJECT

Our WHOLESCALE project has been recommended by the Geothermal Technologies Office of the U.S. Department of Energy for negotiation of a financial award[1]. Indeed, the WHOLESCALE acronym stands for "Water & Hole Observations Leverage Effective Stress Calculations And Lessen Expenses".

The goal of the WHOLESCALE project is to simulate the spatial distribution and temporal evolution of stress in a geothermal system. To reach this goal, the WHOLESCALE team proposes to develop a methodology that will incorporate and interpret data from four methods of measurement into a multi-physics model that couples thermal, hydrological, and mechanical (T-H-M) processes over spatial scales ranging from the diameter of a borehole (~0.1 m) to the extent of the entire field (~10 km) and temporal scales ranging from the duration of a micro-seismic event (~1 second) to the typical lifetime of a producing field (3 decades).

The WHOLESCALE team will take advantage of the perturbations created by pumping operations to infer temporal changes in the state of stress in the geothermal system. This rheological experiment will apply the key idea that increasing pore-fluid pressure reduces the effective normal stress acting across preexisting faults. Accordingly, the WHOLESCALE team proposes to collect four types of observational data at San Emidio:

(1) Seismology will determine the locations and focal mechanisms of micro-seismic events. A dense array of 3-component seismic instruments will be deployed over the area of the 2016 events during the next planned shutdown of the production wells. Seismic tomography — when combined with density models estimated from gravimetric surveys — will also provide constraints on material properties such as Poisson's ratio and shear modulus.

(2) Borehole image logs will observe failures in the formation surrounding the well bore to constrain the magnitude and orientation of stress (e.g., Zoback, 2007). If a given fracture is hydraulically conductive, then we infer that it is active under the current state of stress.

(3) Geodesy will measure deformation of the ground surface. At least two continuously operating GPS stations will be installed, one within the subsiding area and one on stable rock outside it. InSAR monitoring will continue.

(4) Hydrology will measure pressure and temperature in multiple boreholes to quantify the propagation of fluid-pressure fronts and changes to effective normal stress.

Each of these four types of observational data is described in detail below. To interpolate and interpret these rich data sets, the WHOLESCALE team will solve the coupled differential equations governing the physics of a fractured, poroelastic medium under stress. We will perform thermo-hydro-mechanical (T-H-M) coupled modeling using a numerical simulator named GEOS [*Liu et al.*, 2018]. Using a combination of the finite-element and finite-volume methods, the GEOS code solves the coupled differential equations governing the flow of fluid and heat as well as the mechanics of the medium deforming under stress. The resulting solution includes the complete stress tensor σ_{ij} as a function of time t at every location (x, y, z) in a large 3-dimensional mesh of the study volume.

[1] https://www.energy.gov/eere/articles/energy-department-awards-7-million-research-subsurface-stress-and-lost-circulation

In configuring the T-H-M models, the WHOLESCALE team will honor the geologic structure and its material properties. The rock mechanical properties (e.g., Poisson's ratio, density, Young's modulus, thermal expansion coefficient, friction coefficients, effective pressure coefficients) will be measured in samples via laboratory experiments. To account for heterogeneities in mechanical properties over the scale of the reservoir, the WHOLESCALE team will extend the values measured in the lab with information from the borehole logs and the geologic model [*Rhodes*, 2011] using data-science techniques [e.g., *Bayuk et al.*, 2008]. The GEOS code can account for fluid flow in a porous medium that also includes discrete fractures.

The study site at San Emidio includes a volume with length of ~6 km, width ~5 km, and depth ~2 km. At each point within a mesh of this volume, the resulting numerical solution will determine the complete stress tensor as a function of time as well as its sensitivity to perturbations in the input parameters. The numerical GEOS solution will also calculate modeled values for each of the four types of observable quantities. By optimizing the goodness of fit between the observations and the modeled value calculated by the GEOS simulator, the proposed methodology will seek the model configuration that best fits the data while assessing the uncertainty of the associated reservoir parameters. The result will be a reliable simulation of the spatial distribution and temporal evolution of the full stress tensor $\sigma_{ij}(t, x, y, z)$ at San Emidio.

3. EXISTING DATA SETS

Seismology

The study area at San Emidio has been seismically imaged using a temporary array deployed in October 2016. The locations of micro-seismic events and the distribution of emitted seismic energy have been determined [*Warren et al.*, 2018].

Geodesy

Interferometric analysis of synthetic aperture radar images (InSAR) is a geodetic technique that calculates the interference pattern caused by the difference in phase between two images acquired by a satellite radar sensor at two distinct times. The resulting interferogram is a contour map of the change in distance between the ground and the radar instrument. These maps provide a spatial sampling density of ~100 pixels/km^2, a precision of ~10 mm, a registration accuracy of ~10 m, and an observation cadence of ~1 pass/week [e.g., *Massonnet and Feigl*, 1998].

Downward deformation of the ground surface (subsidence) associated with geothermal production can be caused by a number of processes, including contraction due to reductions in pore-fluid pressure, thermally-induced contraction, and/or compaction. The same processes can also change the state of stress in the rock matrix sufficiently to induce failure and thus seismicity. At Brady Hot Springs, subsidence rates as high as 20 mm/yr have been measured using InSAR [*Ali et al.*, 2016]. The process driving the observed subsidence is most likely thermal stress caused by injection of cooled brine, based on Bayesian inference with inverse modeling of the InSAR data [*Reinisch et al.*, 2018].

At San Emidio, subsidence at a rate of several mm/yr was measured in the 1990s using InSAR [*Eneva et al.*, 2011; *Reinisch*, 2019]. For example, Figure 5 shows subsidence at a rate of at least 7 mm/yr at San Emidio. Using nonlinear inversion, *Reinisch et al.* [2019] "determine that the deformation at San Emidio is well explained by parameterizing the reservoir as a cuboidal sink." Furthermore, "temporal analysis of the volume change rates estimated from individual interferometric pairs using this deformation model suggests a constant rate of volume change of $(-1.1 \pm 0.1) \times 10^4$ m^3/yr between 1992 and 2010, consistent with the time-series analysis in terms of line-of-sight displacement performed by Eneva *et al.* [12]." [*Reinisch et al.*, 2019].

Hydrology

Using absolute stress to predict effective stress acting on failure surfaces requires an understanding of the fluid pressure and its evolution over time. These predictions of fluid pressure, in turn, require an understanding of the subsurface permeability structure that determines subsurface flow pathways and pressure propagation.

Existing evidence from San Emidio indicates that the subsurface is highly heterogeneous and that the fluid-flow pathways are likely controlled by faults, similarly to the permeability structure mapped at Brady during the PoroTomo project [*Patterson*, 2018]. For example, spatial heterogeneity of permeability can effect fluid flow. Using pumping well records provided by Ormat, we have developed a simple homogeneous analytical model and estimated permeability and storage coefficients by fitting data from a single observation well at San Emidio. However, when performing forward modeling for a second observation well at San Emidio and using the obtained reservoir parameters, a poor match to pressure data was obtained, indicating the influence of heterogeneity.

We plan to image heterogeneity in aquifer permeability using hydraulic tomography, in which pressure-change measurements from a series of pumping tests are recorded at multiple monitoring wells. Then the complete resulting dataset is inverted via a highly parameterized heterogeneous flow model. Observations are available from several existing wells at San Emidio, and additional instrumentation will be installed in other wells as part of the proposed study. We will use changes in flow rates at operational site wells as the impulses consisting of: (1) ceasing all pumping at all wells; (2) restarting pumping operations; (3) pulsed changes to flow rates at individual injection wells; and (4) returning to normal operations.

Borehole indicators of stress

Although limited in spatial extent, boreholes provide direct access to geological and geophysical information used to construct the numerical model and validate the outcomes of the model. Figure 6 shows a resistivity image log collected in an existing well at San Emidio. As evident from the static image (to the right), the change in lithology from the sediments to the underlying andesite is identified by the shallowly dipping plane and change in appearance. Beneath the lithological boundary is a dark, steeply dipping feature resembling the presence of a large-aperture fluid-filled conductive fracture. As these examples illustrate, borehole images provide crucial information about the distribution of fracture orientation, frequency, and its hydraulic state (open conductive vs. healed/sealed).

Borehole images also provide important constraints on the in-situ stress state at the wellbore location. Open conductive fractures gain conductivity because of dilatancy associated with shear slip along the fracture. Since fractures slip only if favorably oriented under the current state of stress, orientation distributions of open and closed fractures provide constraints on the in-situ stress state [*Zoback*, 2007]. When appropriate stress conditions are met, stress concentrations around the wellbore will create wellbore failures which can also be used to constrain the in-situ stress state at the observed position [*Zoback*, 2007]. We will also perform laboratory testing of available samples to determine material properties such as density, Young's modulus, and Poisson's ratio. In addition, we will determine the frictional properties that govern the sliding strength of faults and fractures as well as thermal and poroelastic properties that control the stress response of rocks to fluid flow and heat transfer. All of these properties are essential for constraining the numerical modeling.

Analysis of the local stress field in the San Emidio area, based on slip indicators along surface-exposed fault planes, reveals an extensional stress regime with a generally west-northwest trending least principal stress [*Rhodes et al.*, 2010; *Rhodes*, 2011](Rhodes, 2011). While this inferred stress is consistent with the normal-faulting system developed in San Emidio and was responsible for the structural development of the field, substantial changes has likely been introduced locally due to heat production in the last two decades. We plan to analyze the available borehole geophysical logs (e.g. gamma ray, density, resistivity, sonic velocity) at San Emidio. These results will help constrain the initial condition of the numerical model before the simulated shut-down of the pumping operations power plant.

4. CONCLUSION

When comparing cumulative volume change estimated from InSAR data at San Emidio to the cumulative gross production recorded by the operators, we find a strong, positive correlation. "This suggests that deformation at San Emidio was influenced by geothermal production at the site between 1998 and 2010" [*Reinisch et al.*, 2019]. As part of the WHOLESCALE project, we will assess the contribution of pressure changes within the modeled reservoir to both vertical deformation (subsidence) and induced seismicity.

The WHOLESCALE project should make an important impact because geothermal operators need quantitative information about the subsurface stress to successfully develop and sustainably manage a geothermal reservoir. The proposed methodology will advance capabilities "to directly measure or infer the stress state" which, as noted in the FOA, "are woefully inadequate, especially away from boreholes" [*EERE*, 2019]. By reducing the uncertainty of in-situ stress estimates, the WHOLESCALE project should reduce the cost of geothermal energy.

5. FIGURES

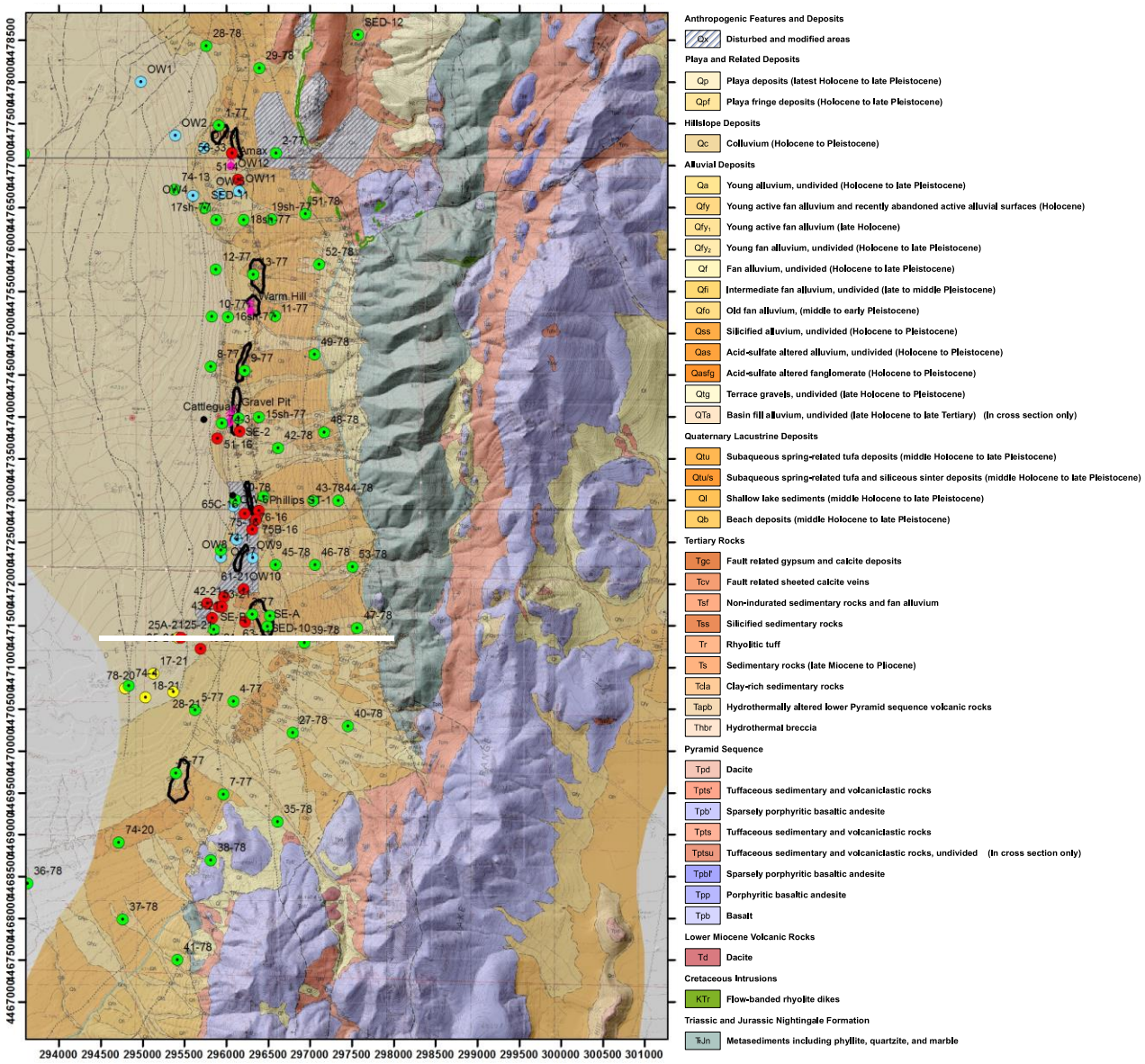

Figure 1. Geologic map of San Emidio [*Rhodes*, 2011], showing lithology [*Rhodes et al.*, 2011], and transect (white line segment). Coordinates are easting and northing in meters in the Universal Transverse Mercator (UTM) cartographic projection. Circles show wells.

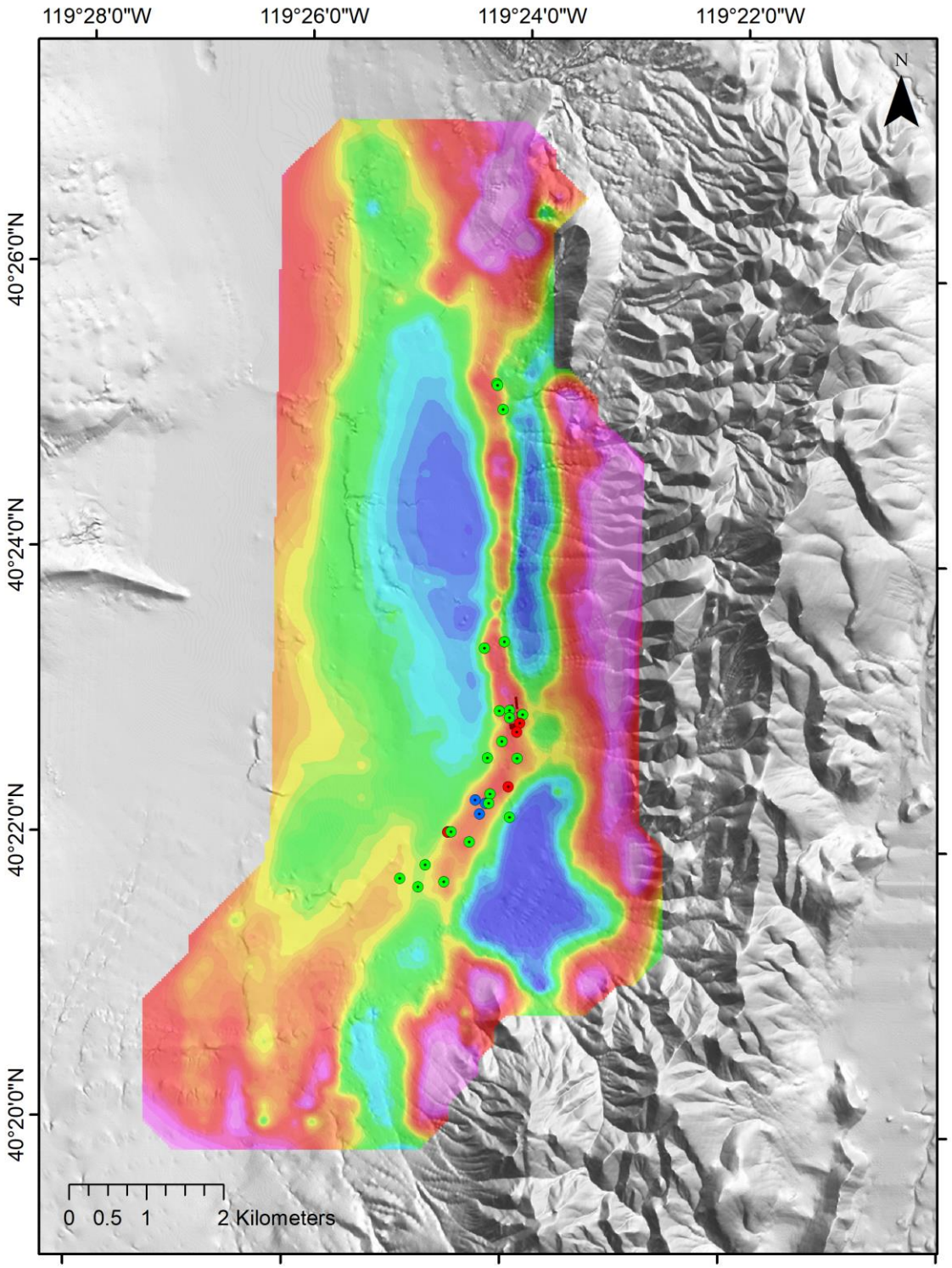

Figure 2. Map of vertical derivative of complete Bouguer gravity anomaly (colors), reduced with density of 2.3 g/cm3 and gridded at 30 m [*Folsom et al.*, 2020]. Gray shading shows topographic relief. Black square shows power plant.

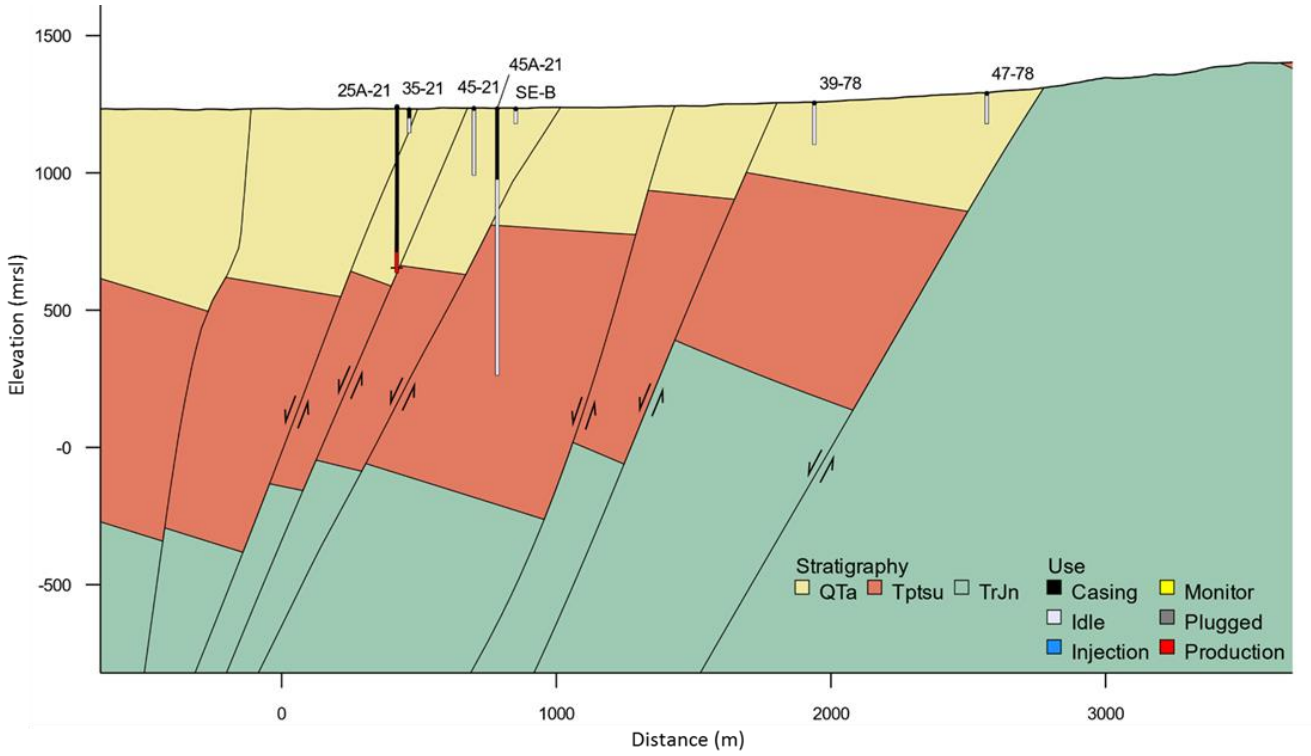

Figure 3. Geologic cross section, showing primary lithologic units, wells, and faults. Vertical plane parallels an E-W transect (white segment in Figure 1). Elevation relative to sea level in meters. Figure copyright © Ormat Technologies, Inc., used by permission.

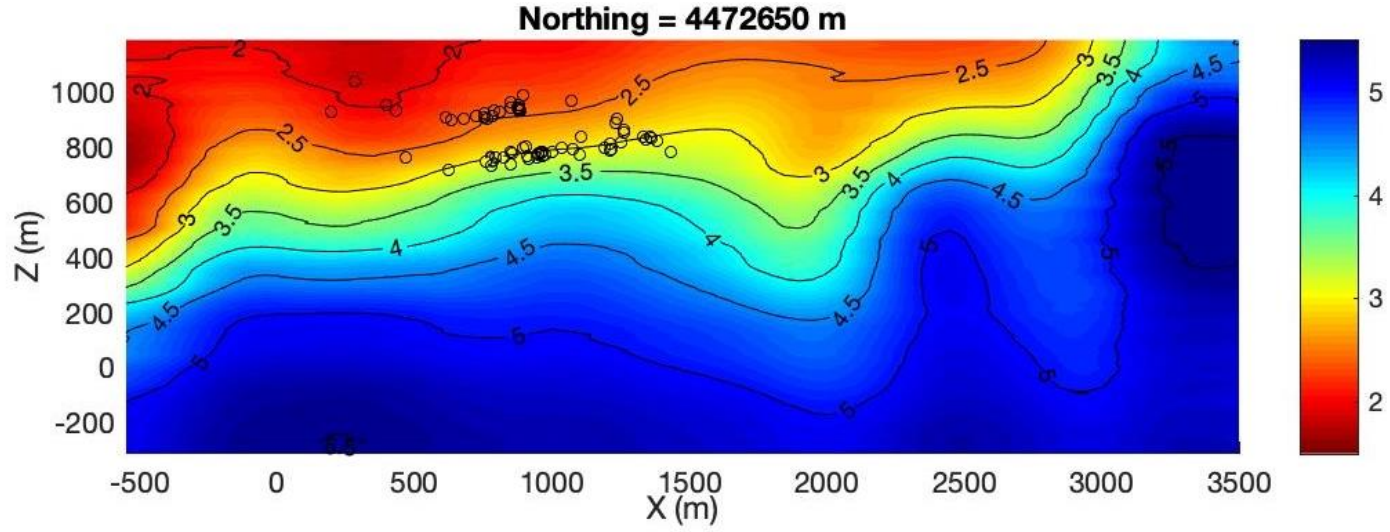

Figure 4. Seismic cross section, showing P-wave velocity in km/s (colors) and microseismic events (black circles). Vertical plane parallels an E-W transect (white in Figure 1). Z = masl. Data from Warren et al. [2018].

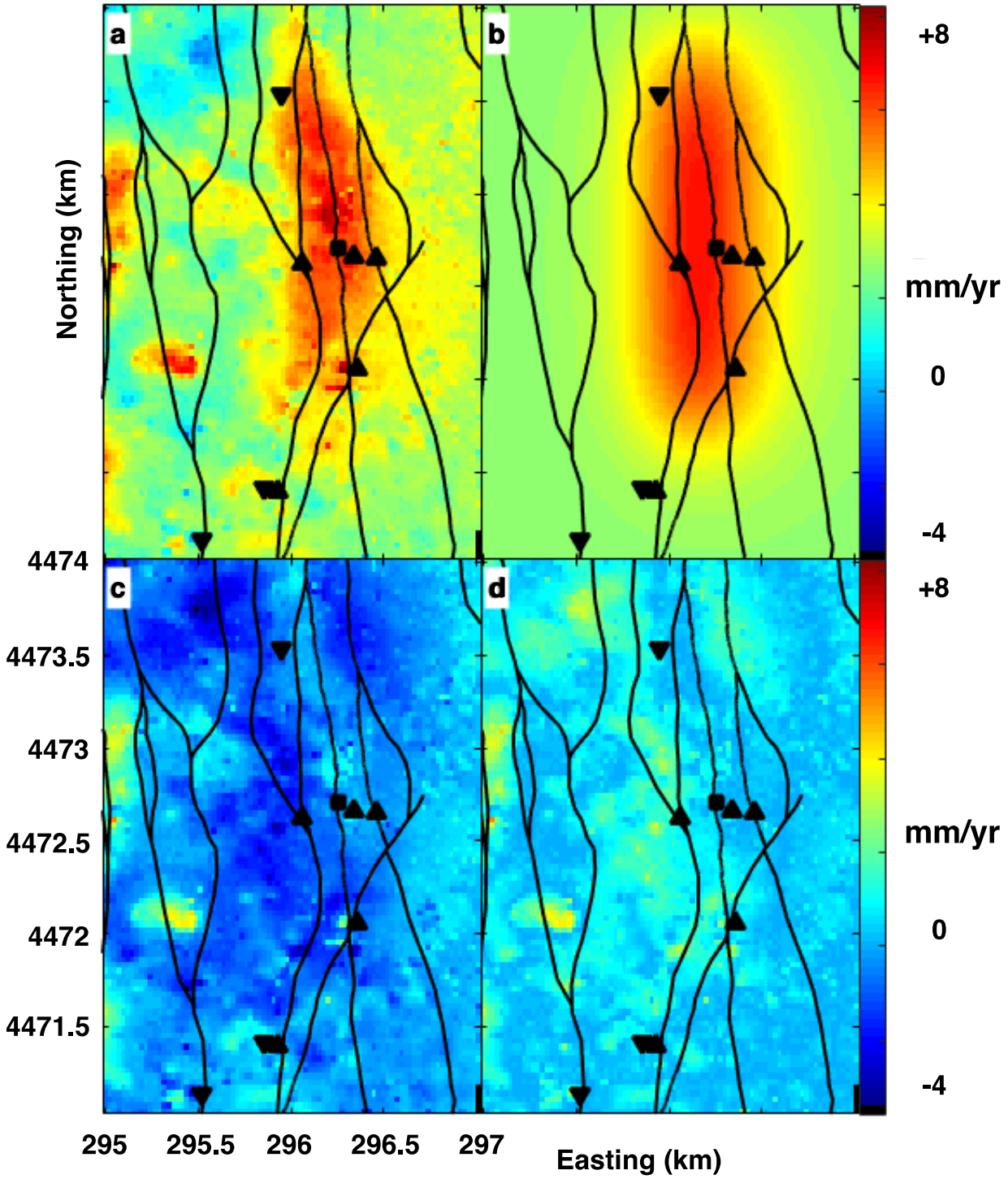

Figure 5. Deformation fields in terms of (unwrapped) range change rate from InSAR data spanning 2004-Jun-23 to 2010-Apr-28 analyzed using nonlinear inversion methods, showing: (a) observed range change rate, (b) modeled range change rate, (c) residual between observed and modeled, and (d) absolute value of residuals. Faults are denoted with black lines. Inverted triangles are injection wells and upright triangles are production wells. The power plant is denoted with a black square. Coordinates are easting and northing [km] in Universal Transverse Mercator (UTM) projection zone 11N, WGS84. Figure from Reinisch et al. (2019).

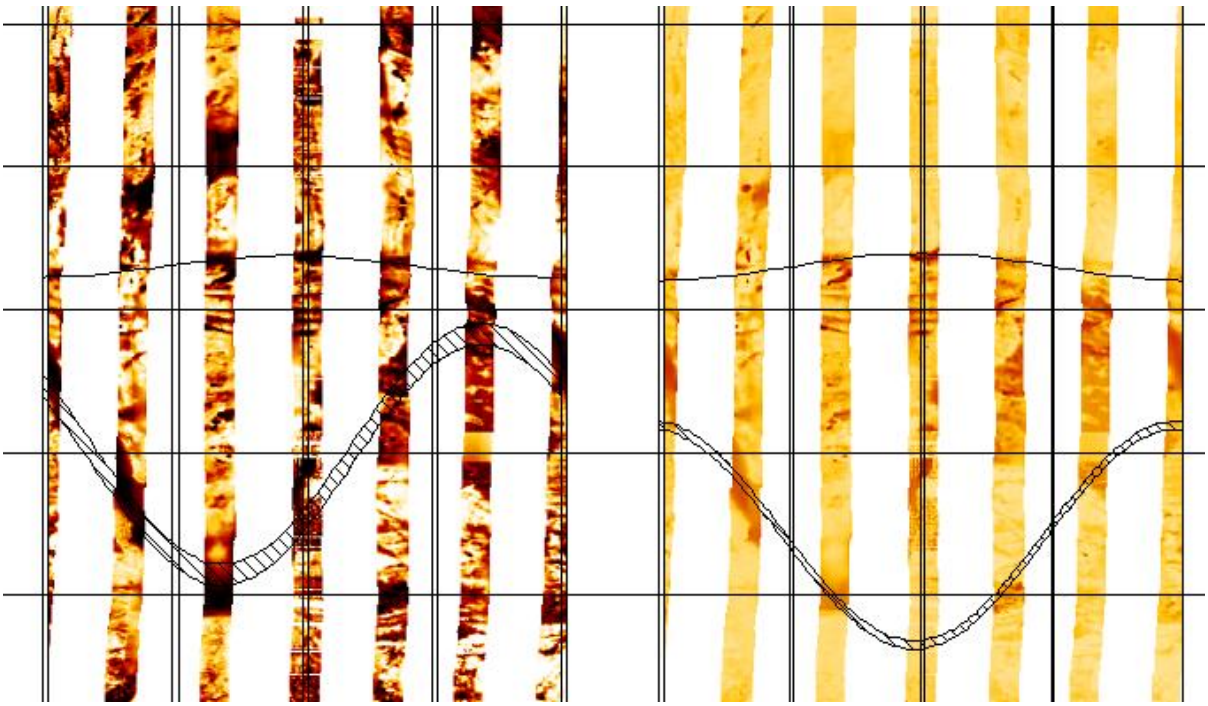

Figure 6. Borehole image of San Emidio Well 25A-21, as logged by a STAR resistivity tool showing the unconformity between the basin sediments and the underlying andesite formation (upper solid black line), and the presence of a conductive fracture (double black line) responsible for the lost circulation observed in this well. Left panel shows the "dynamic" (enhanced contrast) image and right panel shows the "static" (standard contrast). Horizontal lines are separated by ~1.5 meters in depth. Azimuthal orientation is arbitrary.

6. ACKNOWLEDGMENTS

Raw Synthetic Aperture Radar (SAR) data from the Envisat satellite mission operated by the European Space Agency (ESA) are copyrighted by ESA and were provided through the WInSAR consortium at the UNAVCO facility. Raw Synthetic Aperture Radar (SAR) data from the Sentinel-1A satellite mission operated by ESA were available free of charge through the Distributed Active Archive Center (DAAC) at the Alaska Satellite Facility (ASF) and through the Sentinels Scientific Data Hub. This material is based on data services provided by UNAVCO through the GAGE Facility with support from the National Science Foundation (NSF) and National Aeronautics and Space Administration (NASA) under NSF Cooperative Agreement No. EAR-1261833.

Synthetic Aperture Radar data from the TerraSAR-X and the TanDEM-X satellite missions [*Pitz and Miller*, 2010] operated by the German Space Agency (DLR) were used under the terms and conditions of Research Project RES1236. Interferograms were created using GMT-SAR processing software [*Sandwell et al.*, 2011].

Software is available publicly on GitHub for the General Inversion of Phase Technique (GIPhT) [*Feigl et al.*, 2019], the PoroTomo project [*Reinisch and Feigl*, 2018], and the UW Madison HTCondor InSAR Workflow [*Reinisch et al.*, 2018]. Several figures were created using the Generic Mapping Tools [*Wessel et al.*, 2013].

We gratefully acknowledge support from the Weeks family to the Department of Geo- science at the University of Wisconsin-Madison. Research was partially supported by the U.S. Department of Energy under grant DE-EE0007080. Elena C. Reinisch was supported by grants from National Science Foundation Graduate Research Fellowship (DGE-1256259) and the Graduate School at UW-Madison.

7. REFERENCES

Ali, S. T., J. Akerley, E. C. Baluyut, M. Cardiff, N. C. Davatzes, K. L. Feigl, . . . E. Zemach (2016), Time-series analysis of surface deformation at Brady Hot Springs geothermal field (Nevada) using interferometric synthetic aperture radar, *Geothermics, 61*, 114-120. http://dx.doi.org/10.1016/j.geothermics.2016.01.008

Bayuk, I. O., M. Ammerman, and E. M. Chesnokov (2008), Upscaling of elastic properties of anisotropic sedimentary rocks, *Geophys. J. Int., 172*, 842-860. https://doi.org/10.1111/j.1365-246X.2007.03645.x

Brodsky, E. E., and L. J. Lajoie (2013), Anthropogenic Seismicity Rates and Operational Parameters at the Salton Sea Geothermal Field, *Science*. http://dx.doi.org/10.1126/science.1239213

Cardiff, M., D. D. Lim, J. R. Patterson, J. Akerley, P. Spielman, J. Lopeman, . . . K. L. Feigl (2018), Geothermal production and reduced seismicity: Correlation and proposed mechanism, *Earth and Planetary Science Letters, 482*, 470-477. https://doi.org/10.1016/j.epsl.2017.11.037

EERE (2019), Subsurface Stress and Lost Circulation in Geothermal Drilling Funding Opportunity Announcement (FOA) Number DE-FOA-0002083. https://eere-Exchange.energy.gov

Ellsworth, W. L. (2013), Injection-induced earthquakes, *Science, 341*, 1225942. http://www.ncbi.nlm.nih.gov/pubmed/23846903

Eneva, M., G. Falorni, W. Teplow, J. Morgan, G. Rhodes, and D. Adams (2011), Surface Deformation at the San Emidio Geothermal Field, Nevada, from Satellite Radar Interferometry, *GRC Transactions, 35*.

Feigl, K. L., L. M. Parker, and P. Team (2019), PoroTomo Final Technical Report: Poroelastic Tomography by Adjoint Inverse Modeling of Data from Seismology, Geodesy, and Hydrology United States. https://www.osti.gov/servlets/purl/1499141

Folsom, M., R. Libbey, D. Feucht, W. I., and S. Garanzini (2020), Geophysical Observations and Integrated Conceptual Models of the San Emidio Geothermal Field, Nevada. , paper presented at Workshop on Geothermal Reservoir Engineering, Stanford, California, USA.

Kwiatek, G., P. Martínez- Garzón, G. Dresen, M. Bohnhoff, H. Sone, and C. Hartline (2015), Effects of long- term fluid injection on induced seismicity parameters and maximum magnitude in northwestern part of The Geysers geothermal field, *Journal of Geophysical Research: Solid Earth, 120*, 7085-7101. https://agupubs.onlinelibrary.wiley.com/doi/abs/10.1002/2015JB012362

Liu, F., P. Fu, R. J. Mellors, M. A. Plummer, S. T. Ali, E. C. Reinisch, . . . K. L. Feigl (2018), Inferring Geothermal Reservoir Processes at the Raft River Geothermal Field, Idaho, USA, Through Modeling InSAR-Measured Surface Deformation, *Journal of Geophysical Research: Solid Earth, 123*, 3645-3666. http://dx.doi.org/10.1029/2017JB015223

Majer, E. L., R. Baria, M. Stark, S. Oates, J. Bommer, B. Smith, and H. Asanuma (2007), Induced seismicity associated with enhanced geothermal systems, *Geothermics, 36*, 185-222.

Massonnet, D., and K. L. Feigl (1998), Radar interferometry and its application to changes in the Earth's surface, *Rev. Geophys., 36*, 441-500. http://dx.doi.org/10.1029/97RG03139

McGarr, A., B. Bekins, N. Burkardt, J. Dewey, P. Earle, W. Ellsworth, . . . A. Sheehan (2015), Coping with earthquakes induced by fluid injection, *Science, 347*, 830-831. http://www.sciencemag.org/content/347/6224/830.full.pdf

NRC (2013), *Induced Seismicity Potential in Energy Technologies*, National Acad. Press, Washington, D. C.

Patterson, J. R., M. Cardiff, T. Coleman, H. Wang, K. L. Feigl, J. Akerley, and P. Spielman (2017), Geothermal reservoir characterization using distributed temperature sensing at Brady Geothermal Field, Nevada, *The Leading Edge, 36*, 1024a1021 - 1024a1027. http://dx.doi.org/10.1190/tle36121024a1.1

Patterson, J. R. (2018), Understanding Constraints on Geothermal Sustainability Through Reservoir Characterization at Brady Geothermal Field, Nevada, M.S. thesis, University of Wisconsin-Madison (M. Cardiff, advisor).

Raleigh, C. B., J. H. Healy, and J. D. Bredehoeft (1976), An experiment in earthquake control at rangely, colorado, *Science, 191*, 1230-1237. http://www.ncbi.nlm.nih.gov/pubmed/17737698

Reinisch, E. C., M. Cardiff, and K. L. Feigl (2018), Characterizing Volumetric Strain at Brady Hot Springs, Nevada, USA Using Geodetic Data, Numerical Models, and Prior Information, *Geophys. J. Int.*, 1501–1513. http://dx.doi.org/10.1093/gji/ggy347

Reinisch, E. C. (2019), Spatio-temporal Characterization of Geothermal Fields by Inverse Modeling, University of Wisconsin-Madison advisor).

Reinisch, E. C., M. Cardiff, J. Akerley, I. Warren, and K. L. Feigl (2019), Spatio–Temporal Analysis of Deformation at San Emidio Geothermal Field, Nevada, USA Between 1992 and 2010, *Remote Sensing, 11*, 1935. http://dx.doi.org/10.3390/rs11161935

Rhodes, G. T., J. E. Faulds, and W. Teplow (2010), Structural Controls of the San Emidio Desert Geothermal Field, Northwestern Nevada, paper presented at Geothermal Resource Council Transactions.

Rhodes, G. T. (2011), Structural controls of the San Emidio Geothermal System, M.S. thesis, vi, 73 leaves pp, University of Nevada Reno advisor).

Rhodes, G. T., J. E. Faulds, and A. R. Ramelli (2011), Preliminary Geologic Map of the Northern Lake Range, San Emidio Geothermal Area, Washoe County, Nevada Nevada Bureau of Mines and Geology

Segall, P., and S. Lu (2015), Injection-induced seismicity: Poroelastic and earthquake nucleation effects, *Journal of Geophysical Research: Solid Earth, 120*, 5082-5103. http://dx.doi.org/10.1002/2015jb012060

Teplow, W. J., and I. Warren (2015), Finding Large Aperture Fractures in Geothermal Resource Areas Using a Three-Component Long-Offset Surface Seismic Survey, PSInSAR and Kinematic Structural Analysis, Medium: ED; Size: 52 p. pp, US Geothermal, Inc., Boise, ID (United States). https://doi.org/10.2172/1213113

Trugman, D. T., P. M. Shearer, A. A. Borsa, and Y. Fialko (2016), A comparison of long-term changes in seismicity at The Geysers, Salton Sea, and Coso geothermal fields, *Journal of Geophysical Research: Solid Earth, 121*, 225-247. http://dx.doi.org/10.1002/2015jb012510

Warren, I., E. Gasperikova, S. Pullammanappallil, S. S, and M. Grealy (2018), Mapping Geothermal Permeability Using Passive Seismic Emission Tomography Constrained by Cooperative Inversion of Active Seismic and Electromagnetic Data, paper presented at Proceedings, 43rd Workshop on Geothermal Reservoir Engineering Stanford University, Stanford, California, 2018 SGP-TR-213, February 12-14, 2018.

Zoback, M. D. (2007), *Reservoir geomechanics*, Cambridge University Press.